Carbon and Oxygen Levels in Nitinol Alloys and the Implications for Medical Device Manufacture and Durability

Morgan, Wick, DiCello, Graham

Proceedings of the International Conference on Shape Memory and Superelastic Technologies, SMST-2003

2006

Carbon and Oxygen Levels in Nitinol Alloys and the Implications for Medical Device Manufacture and Durability

Neil Morgan
Point Technologies (an Angiotech Company), Boulder, CO 80302

Andreas Wick, John DiCello
Nitinol Devices and Components, 47533 Westinghouse Dr., Fremont, CA 94539

Ron Graham
ATI Wah Chang, 1600 N.E. Old Salem Road, Albany, OR 97321

Abstract

This paper will consider the impact of carbon and oxygen content on Nitinol for medical applications. Three Nitinol melts were chosen to yield varying levels of oxygen and carbon content and were subsequently drawn to yield representative wire and tubing sizes for typical medical device applications. Inclusion content was studied via scanning electron microscopy and a series of fatigue and processing trials were carried out in order to study their effect.

Introduction

The increasing number of permanently implanted devices employing Nitinol places great demands on manufacturing quality and on in vivo fatigue life. In the past, inclusion content within Nitinol has often been linked to low process yields and fatigue crack initiation. While several studies have attempted to link the presence, size and distribution of inclusions with fatigue life [1-3], none have reached definitive conclusions regarding their effect.

The following paper reports on the results of a systematic study on the effect of different melt methods and their associated inclusion content on fatigue life and Nitinol component manufacture.

Materials

Melting techniques for NiTi include either multiple vacuum arc remelts (VAR), or a vacuum induction melt (VIM) process followed by VAR. The combination of the VIM and the VAR process will be referred to as VIM/VAR. The standard VAR process (VAR-Standard) is a series of four successive melts into increasingly larger water-cooled copper crucibles, ending with a finished ingot of 585 mm diameter. Input materials for the standard practice include alloy grade, Kroll-reduced, titanium sponge and electrolytic nickel. The electrode is made by standard compaction and welding techniques. This practice has proved to produce good homogeneity and reasonably uniform Af temperatures for large- scale (3,000 kg) ingots. The VAR-ELI (Extra Low Inclusion) process incorporated three melts to finish with a 405 mm diameter ingot. Input materials for the ELI ingot included iodide-reduced titanium crystal bar produced by a Van Arkel-

deBoer process, and electrolytic nickel. A special construction method was used to produce the electrode for the ELI first-melt ingot.

The Nitinol alloys used for this study were purchased on the open market. The alloys were produced using these three different melt methods:
- VAR-Standard
- VAR-ELI
- VIM/VAR

The chemical composition in weight percent of each melt is shown below in Table 1, the carbon and oxygen levels are highlighted in bold as these are most significant for inclusion content. As a reference the allowable limits per ASTM standard F2063-00 are given in the table as well.

Table 1: Chemical Analysis of the three differnet melts. The allowable limits per ASTM F2063-00 are given as a reference

	ASTM F2063-00	VAR-Standard	VAR-ELI	VIM/VAR
Ni	54.5-57.0	55.6	55.3	54.5
Ti	balance	44.3	44.6	45.3
Al	N/A	0.0075	0.0053	0.010
Cu	0.010max	0.0049	0.0027	0.0063
Cr	0.010max	0.0036	0.008	0.004
Fe	0.050max	0.014	0.020	0.030
Nb	0.025max	<0.002	<0.002	<0.002
C	**0.070max**	**0.004**	**0.002**	**0.029**
H	0.005max	0.0007	0.0001	0.0012
O	**0.050max**	**<0.033**	**0.009**	**0.025**
N	N/A	<0.001	<0.001	<0.001

Chemical Analysis Methods:
    Hydrogen: Vacuum hot extraction
    Nitrogen and Oxygen: Inert gas fusion
    Carbon: Combustion infrared detection

Each melt was worked down into 0.6mm wire and tubing with an OD of 1.82mm and an ID of 1.29mm. The Af temperatures for the wires and tubes at final size were determined using a bend and free recovery method according to ASTM standard F2082. Table 2 shows the Af temperatures for all conditions.

Table 2: Af temperatures of the wires and tubes at end size as measured by a bend and free recovery method

	VAR-Standard	VAR-ELI	VIM/VAR
Wire	0°C	- 5°C	+ 1°C
Tube	- 12°C	- 18°C	- 13°C

Experimental

Tensile Properties

The tensile properties of each wire were measured (according to ASTM F2516) at 23°C and are shown below in Table 3. In agreement with its slightly lower Af temperature, the ELI melt wire resulted in the highest upper and lower plateau stresses.

Table 3: Upper and lower plateau values of the different wires measured at 23°C

	VAR-Standard	VAR-ELI	VIM/VAR
Upper Plateau [MPa]	553	609	562
Lower Plateau [MPa]	158	220	152

With a stress gradient of 6.1MPa°C^{-1} [4], a 10°C increase of test temperature for the wires with lower plateau stresses should increase those values to approximately the plateaus values of the ELI wire at 23°C. This is confirmed below in Table 4.

Table 4: Upper and lower plateau values of the different wires measured at 33°C

	VAR-Standard	VAR-ELI	VIM/VAR
Upper Plateau [MPa]	619	N/A	632
Lower Plateau [MPa]	221	N/A	232

Fatigue Properties

The tensile data established the fatigue testing temperatures for each wire thus ensuring equal stress conditions for each alternating strain employed. Table 5 shows the fatigue test temperatures for each wire type.

Table 5: Fatigue test temperatures

	VAR-Standard	VAR-ELI	VIM/VAR
Fatigue test temperature	*33°C*	*23°C*	*33°C*

Wires of each melt were fatigue tested in the unpolished (black oxide surface) and electropolished conditions.

Rotary bending tests were performed using a guided rotary bend tester. This is the same tester that was used for previous studies (e.g. [2]). The specimens were guided around a fixed diameter mandrel. Different mandrel diameters were used in order to produce a range of outer-fiber strains. Strain was estimated with $\varepsilon = r/\rho$ where ε is the strain, r is the radius of the wire and ρ is the radius of curvature of the mandrels used. Test temperatures from 23°C and 33°C were realized with a Haake K15 temperature-control liquid bath. Tests were run until failure was detected or until 10^7 cycles.

Scanning Electron Microscopy

All scanning electron microscopy (SEM) was carried out on a JEOL JSM 5600. Polished cross-sections of wire and tubing were imaged in backscatter compositional (BSE) mode to facilitate inclusion contrast. Component manufacture steps were imaged in BSE and secondary electron (SE) modes.

Component Manufacture Implications

The implications for component manufacture and quality were assessed through the manufacture of laser cut component parts. Tubing from three gun-drilled hollows produced using the three melt methods mentioned above were manufactured. Twenty laser cut components were manufactured from each tubing lot under identical conditions. Each tubing lots came from the same starting melts as the equivalent wire samples used for the fatigue study (compare Table 1).

Results and Discussion

Wire microstructure

Figure 1 shows BSE electron micrographs of polished longitudinal sections of each wire lot used for the fatigue testing. The depth of the polish could not be precisely controlled but the micrographs are taken at the same magnification.
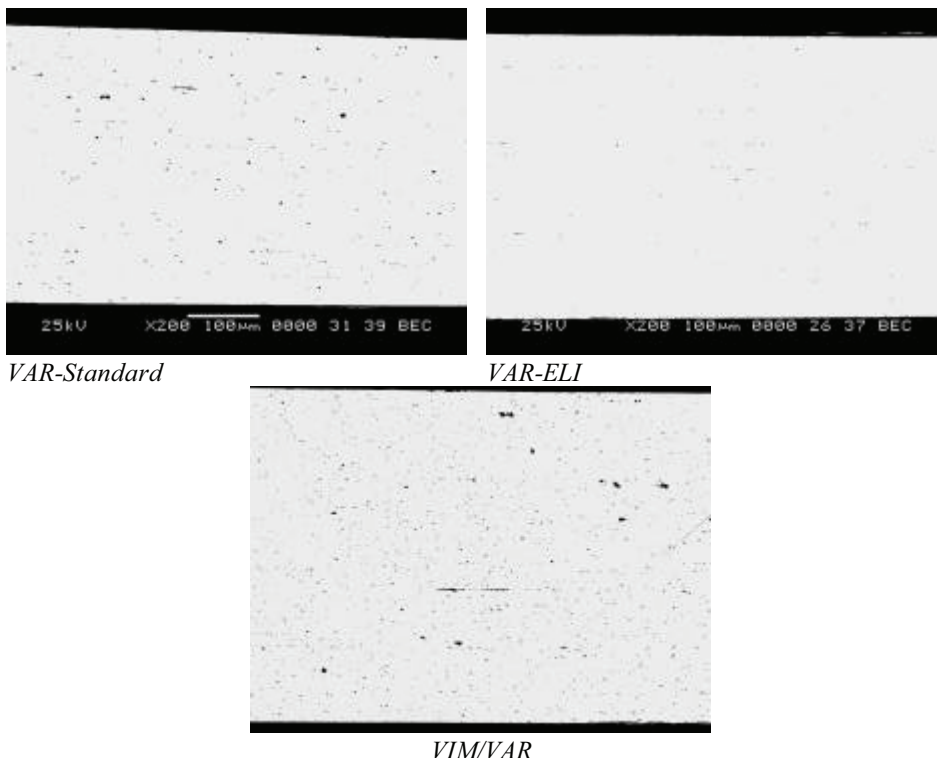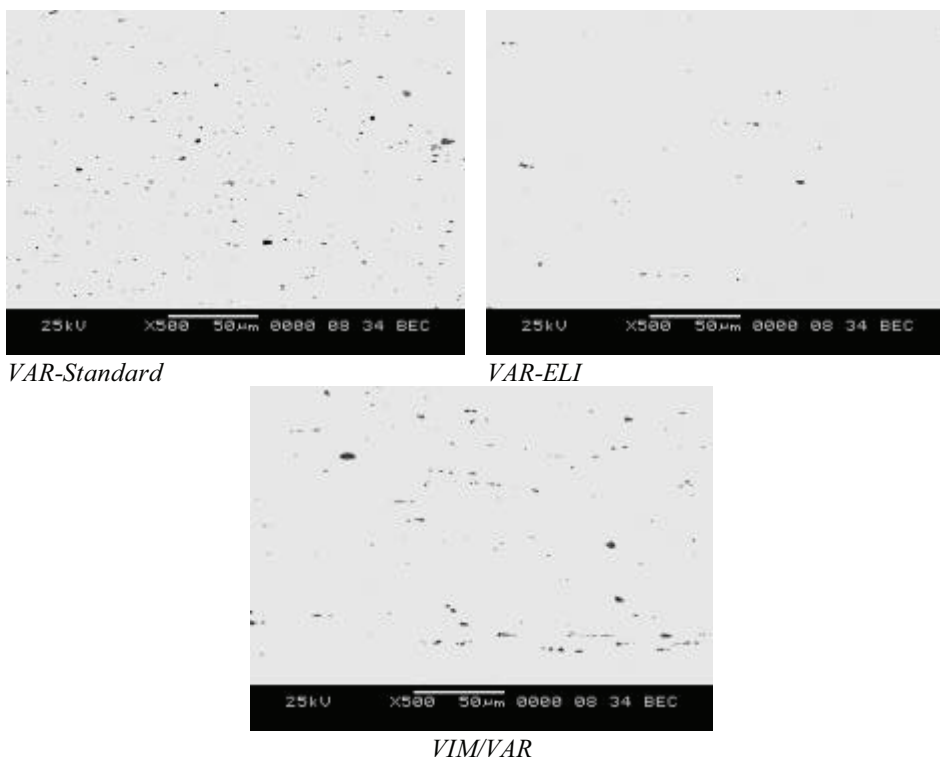

VAR-Standard

VAR-ELI

VIM/VAR

Figure 1: Longitudinal inclusion characterization of wire drawn from each melt method (original magnification: 200x)

Tube microstructure
Figure 2 shows BSE electron micrographs of polished longitudinal sections of each tube lot used for manufacturing the laser cut components.

VAR-Standard   *VAR-ELI*

VIM/VAR

Figure 2: Longitudinal inclusion characterization of tubing drawn from each melt method (original magnification: 500x)

It can be seen that the size of the oxide inclusions for all three materials are approximately the same. All three materials meet the requirements of ASTM-F2063. The ELI material seems to have a substantially lower volume fraction of inclusions than the VAR-Standard and the VIM/VAR material. Due to the higher carbon, the VIM/VAR material shows a significantly higher amount of carbides than the VAR materials.

Fatigue Results
There does not appear to be a significant difference between the different melt Nitinol when tested in the unpolished condition. This can be seen in Figure 3. The fatigue resistance for wires from all three melt methods seem to be comparable. No significant difference can be seen for the three wire lots studied.

However, after electropolishing the wires do appear to display differences in cycles to failure according to the melt method employed. Overall the electropolished wires result in improved fatigue lives for all wires at all strain levels. This emphasizes the importance of surface finish and Nitinol fatigue life (Figure 4).
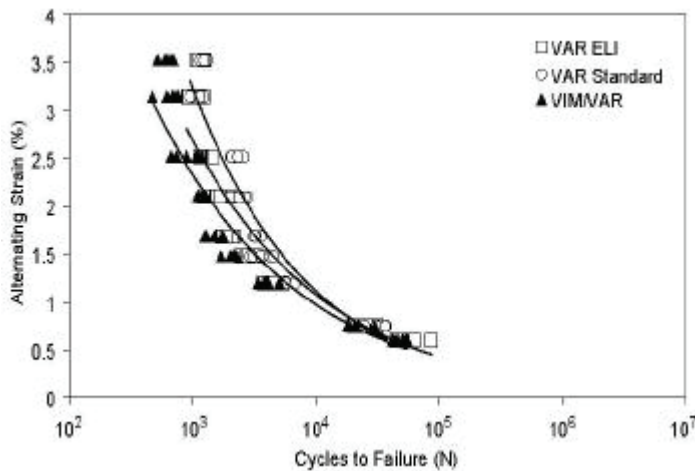
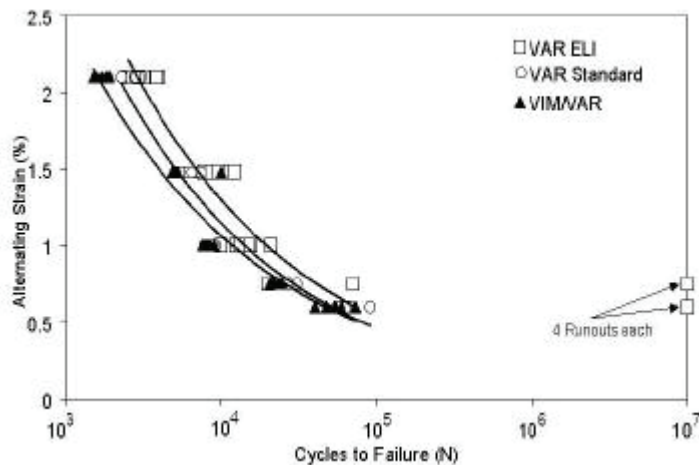*Figure 3: S-N curves for wires with oxide surfaces*

Figure 4: S-N curves for electropolished wires

Based on the limited data collected for this study, the electropolished VAR-ELI melt wires seems to have a marginally improved fatigue life. The data show that for alternating strains above 1.0% the cycles to failure for the ELI material are slightly higher than those for the VAR Standard and the VIM/VAR material. A more significant improvement of the fatigue behavior is observed at alternating strains of 0.75% and 0.6%. In fact, at 0.75% alternating strain four of the ELI samples did not break at 10 million cycles; none of the VAR- Standard or VIM/VAR samples ran out. At 0.6% strain, all the ELI samples ran out to 10^7 cycles, whereas all the Standard VAR and the VIM/VAR samples broke between $4x10^4$ and $9x10^4$ cycles.

It is frequently observed that fatigue cracks tend to initiate at inclusions [1-3]. Therefore, one possible explanation for the improved fatigue performance of the ELI material may be the lower inclusion content.

To get a more complete understanding on the influence of the melting method on the fatigue behavior, more data need to be collected, especially for the VAR-ELI material.

Component Manufacture Implications

During manufacturing, the laser cut components were examined at different stages of the manufacturing process. These included: after laser cutting, after initial expansion etc. No significant differences were found in the response of the various melt methods other than post electropolish when some interesting observations were made. It was clear from examining many different laser cut components from each lot of twenty that the amount of 'pinhole' and pit type defects was greatly reduced in the ELI melt laser cut components.

Figure 5 shows the electropolished surfaces of the various melt method laser cut components. The images on the left hand side (a) are generated using secondary electrons and small surface pits can be seen on the surface of the VIM/VAR and the VAR- Standard Process melt tubing. The VAR-ELI melt laser cut component surface is comparatively free of defects. The right hand images (b) of Figure 5 are generated using backscattered electrons and enhance the contrast between the Nitinol matrix material and the oxide and/or carbide inclusions.
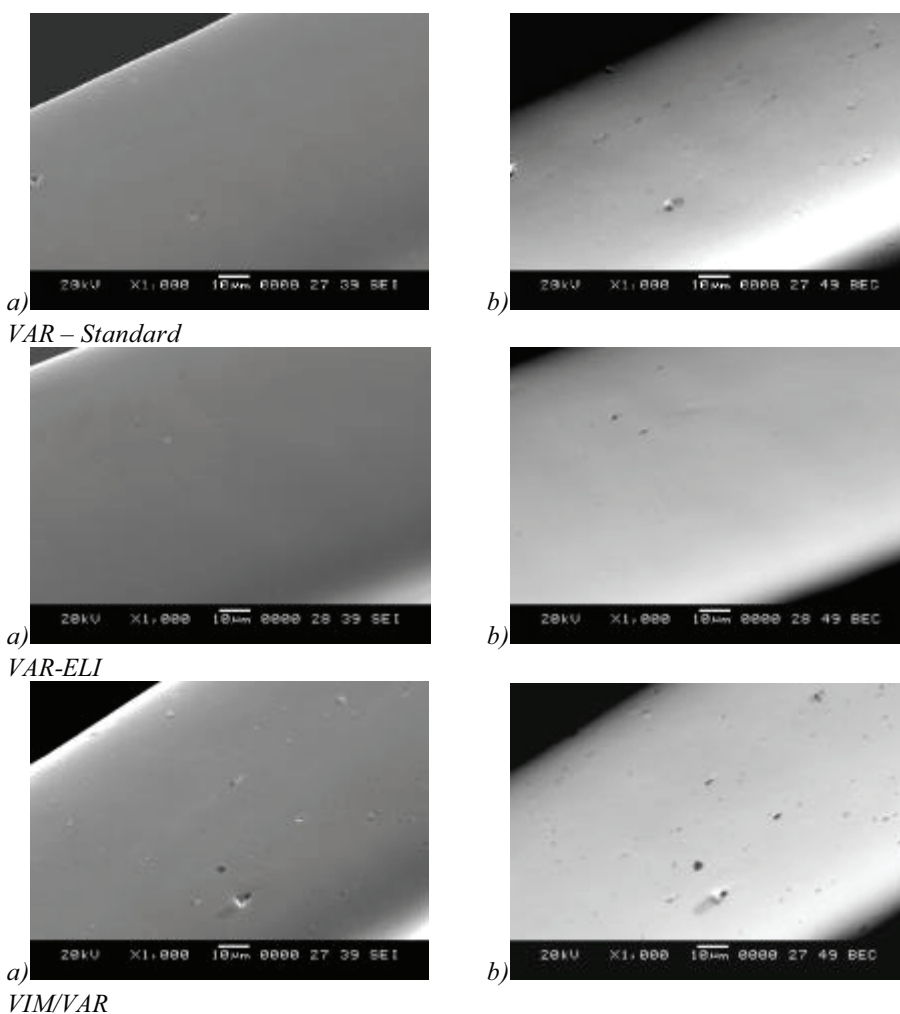

a) *VAR – Standard*

b)

a) *VAR-ELI*

b)

a) *VIM/VAR*

b)

Figure 5: SEM images of component surfaces made from tubing produced with the three different melt techniques. (a) Secondary electron image, b) Backscattered image)

It is clear that the defects observed using secondary electrons are in all cases associated with inclusions. The images are typical of all the laser cut components and laser cut component locations examined.

Conclusions

- Standard Nitinol material (VAR and VIM/VAR) contains high numbers of inclusions within the microstructure while VAR-ELI material contains comparatively few.
- It is frequently observed that fatigue cracks tend to initiate at inclusions this may also explain why VAR-ELI Nitinol appears to result in improved fatigue performance.
- Fewer inclusions (oxides and carbides) appear to increase the strain limit below which fatigue lives greater than 10^7 cycles may be achieved.
- Electropolished surfaces tend to result in greater fatigue lives than unpolished for any given strain level.
- Inclusions frequently lead to pinhole/pit type defects on electropolished surfaces.
- ELI Nitinol results in fewer surface defects after electropolishing. The improvements in electroplished surface finish for ELI Nitinol may reduce fall out during production and therefore may offer greater production yields.

References

[1] M. Reinoehl, *et al*.: "The Influence of Melt Practice on Final Fatigue Properties of Superelastic NiTi Wires", *Proc. SMST 2000, p. 397-403*
[2] R. Graham *et al*.: "Characteristics of High Purity Nitinol", *Proc. SMST 2003, p. 7-14*
[3] S. Miyazaki: "Thermal and Stress Cycling Effects and Fatigue Properties of Ni-Ti Alloys", *Engineering Aspects of Shape Memory Alloys, p. 394-411*
[4] Alan R. Pelton *et al*," Optimization of Processing and Properties of Medical-Grade Nitinol Wire", *Proc. SMST 2000, p. 361-374*